Dynamics of glass-forming liquids. XVI. Observation of ultrastable glass transformation via dielectric spectroscopy

Z. Chen, A. Sepúlveda, M. D. Ediger, and R. Richert

Citation: The Journal of Chemical Physics **138**, 12A519 (2013); doi: 10.1063/1.4771695

View online: http://dx.doi.org/10.1063/1.4771695

View Table of Contents: http://scitation.aip.org/content/aip/journal/jcp/138/12?ver=pdfcov

Published by the AIP Publishing

Dynamics of glass-forming liquids. XVI. Observation of ultrastable glass transformation via dielectric spectroscopy

Z. Chen,[1] A. Sepúlveda,[2] M. D. Ediger,[2] and R. Richert[1,a)]
[1]*Department of Chemistry and Biochemistry, Arizona State University, Tempe, Arizona 85287-1604, USA*
[2]*Department of Chemistry, University of Wisconsin-Madison, Madison, Wisconsin 53706, USA*

(Received 8 October 2012; accepted 28 November 2012; published online 3 January 2013)

The transformation of vapor-deposited ultrastable glasses of indomethacin (IMC) into the supercooled liquid state near T_g is monitored by means of dielectric spectroscopy. Films with thickness between 400 and 800 nm are deposited on differential interdigitated electrode cells and their loss profiles are measured during isothermal annealing using a dual-channel impedance technique for frequencies between 0.03 and 100 Hz. All dielectric loss spectra observed during the transformation process can be explained by a volume fraction of the supercooled liquid that increases linearly with time. From the early stages of the transformation to the liquid that is formed via complete annealing of the ultrastable glass, the average dielectric relaxation time as well as the distribution of relaxation times of the liquid component are identical to those of the conventional liquid obtained by cooling the melt. The dependence of the transformation rate on the film thickness is consistent with a growth front mechanism for the direct conversion from the ultrastable glass to the equilibrium supercooled liquid. We conclude that the IMC liquid recovered from the ultrastable glass is structurally and dynamically identical to the conventional supercooled state. © *2013 American Institute of Physics*. [http://dx.doi.org/10.1063/1.4771695]

I. INTRODUCTION

Glasses of exceptional stability can be prepared by physical vapor deposition (PVD) if appropriate substrate temperatures and deposition rates are used,[1–3] as has been demonstrated for a number of organic molecular glass formers.[1–9] Examples include not only canonical glass formers, such as indomethacin (IMC) and α,α,β-tris-naphthylbenzene (TNB), but also some marginal glass formers.[9] These glassy states prepared by PVD at substrate temperatures around $T_{sub} = 0.85\ T_g$ (generally within hours) possess interesting properties that would otherwise require thousands of years to obtain via cooling the liquid below the glass transition temperature (T_g) and subsequent standard physical aging.[1–3] This has provided the opportunity to study vitreous states that are not accessible via conventional methods on typical laboratory time scales. In order to discriminate among the various states of glass-forming liquids, we use the following terms: "supercooled liquid" for $T > T_g$, "conventional glass" for $T < T_g$ prepared by cooling the melt and aging, and "ultrastable" for designating glasses prepared by PVD with a substrate temperature $T_{sub} \approx 0.85\ T_g$. An increasing number of striking properties are being discovered in these ultrastable glasses,[4–7,10–18] which are significantly different from those of conventional glasses produced by cooling the melt at a few K/min. These properties include higher thermal stability,[7,13] lower heat capacity,[7,10] lower enthalpy,[3,14] higher density,[15] higher mechanical moduli,[16] lower thermal expansion coefficients,[15] higher resistance to vapor uptake,[18] and anisotropic packing.[12,17] Results obtained by varying the substrate temperature between T_g and 0.85 T_g indicate structural continuity between the ordinary and the ultrastable glass.[7,11,14] Apart from a peak indicating some tendency towards molecular layering, these materials show broad wide-angle X-ray scattering (WAXS) patterns that are nearly identical to the conventional glass counterparts, i.e., without sharp peaks characteristic of crystalline materials.[8,12] Some of the above properties have also been produced in computer simulations that model ultrastable glass formation.[19,20]

Additionally, the transformation behavior of ultrastable glasses to the supercooled liquid state is also seen to be very different from their conventional glass counterparts.[10,12,13,21–26] When a conventional glass is isothermally annealed above T_g, it transforms into a supercooled liquid (SCL) if crystallization can be avoided. For conventional glasses, this transformation occurs in a spatially homogeneous manner characterized by a global and gradual softening of the sample.[27–29] Depending on the aging history of the conventional glass, this process typically completes within $3\tau_\alpha$ to $30\tau_\alpha$, with τ_α being the structural relaxation time of the supercooled liquid at the annealing temperature.[30–32] For ultrastable glasses with a thickness below 1 μm, however, it has been found that the transformation is heterogeneous and follows a growth front mechanism. As clearly observed by secondary ion mass spectrometry (SIMS),[21,24,26] the growth front is initiated at the free surface (and sometimes at the substrate/ultrastable glass interface) and subsequently propagates into the bulk with a constant velocity. The transformation times of the ultrastable glasses have been estimated to be more than 3 orders of magnitude longer than τ_α at the transformation temperature.[12]

a)Author to whom correspondence should be addressed. Electronic mail: ranko@asu.edu.

This growth front separates the sample into at least two parts: a liquid part behind the front that has been formed from the ultrastable glass, and a still vitrified and much more efficiently packed part on the other side of the front. Further evidence that supports this transformation behavior comes from differential scanning calorimetry (DSC),[23] quasi-isothermal temperature-modulated DSC,[23] WAXS,[12] and pulse-heating nanocalorimetry.[33] Transformation of ultrastable glasses via a growth front has been modeled by a facilitated kinetic Ising model,[19] and has been predicted on the basis of the random first order transition theory of glasses.[34]

A previous SIMS study indicated that the liquid transformed from ultrastable glasses of IMC and TNB behind the front has a greater mobility than the conventional SCL, with the self-diffusion coefficient D being about 3 times larger.[24] Polyamorphism[35,36] was suggested as one possibility to account for the anomalously fast liquid diffusion. Within this scenario, the fast liquid was regarded as a metastable liquid state that differs from the conventional SCL and a phase transition would be involved in the transformation process. Accordingly, the ultrastable glass would be associated with a structure that differs qualitatively from the conventional SCL counterpart. However, a recent SIMS study[26] on the same ultrastable glasses but with improved deposition procedures indicated that the liquid transformed from the ultrastable glass displays a value of D that is comparable to that of conventional SCL. That study revealed no indication of polyamorphism and suggested that the enhanced mobility observed in the previous SIMS study resulted from low level contaminants during the deposition process. To date, the dynamic features in the course of the transformation from the ultrastable glass to the liquid have been characterized only by SIMS. Therefore, it is highly desirable to have complimentary methods that provide more insight into the properties of the liquid state as it is recovered from an ultrastable glass.

Dielectric spectroscopy is a very advantageous noninvasive technique for monitoring the annealing process of ultrastable glasses,[37,38] partly due to its sensitivity and broad frequency range.[39] Because the transformation times are long compared with the structural or α relaxation time of the conventional liquid at the annealing temperature, the complete loss spectrum can be recorded multiple times in the course of the annealing process. This allows us to follow the relaxation amplitude, the characteristic relaxation time, as well as the shape parameters or dispersion of the dynamics as the system recovers from the ultrastable glass to the liquid state.

We monitored the evolution of the dielectric behavior of ultrastable glasses of IMC during their annealing at several temperatures slightly above the conventional T_g. Already when only one fourth of the sample volume has transformed to the liquid state, the dielectric relaxation spectrum of this component is indistinguishable from that of the conventional supercooled liquid. The linear increase of the liquid volume fraction in time is consistent with recent SIMS results and provides further evidence of a growth front mechanism that converts the ultrastable glass directly to the supercooled liquid. Accordingly, no indications for a metastable state of IMC that differs from the regular supercooled state for $T > T_g$ are found, given the present experimental conditions.

II. EXPERIMENTAL

IMC was purchased from Sigma-Aldrich, with purity greater than 99%. Ultrastable IMC glass films were prepared by means of PVD. Details on the deposition procedure onto the interdigitated electrode (IDE) cells (ABTECH Scientific, Inc.)[40,41] have been reported previously.[42] The base pressure inside the PVD chamber was 5×10^{-8} torr. The deposition rate and temperature were held constant at 0.2 nm/s and 265 K (0.85 T_g), respectively. The rates and thicknesses were monitored by a quartz crystal microbalance. After deposition, the samples were removed from the PVD chamber and stored at a temperature below 258 K until the dielectric measurements were performed. The three types of film structures investigated in this study are represented schematically in Fig. 1.

Isothermal dielectric measurements were carried out with a dual-channel impedance measurement setup coupled with a differential IDE cell. The measurement protocol and data analysis method of the dual-channel impedance measurement have been detailed previously.[42] The purpose of the dual-channel approach is to measure the substrate signal of the IDE in a separate channel for subtraction so that the permittivity of the sample itself can be derived from the IDE impedance data. Prior to the dielectric measurement, the differential IDE cell with one IDE loaded with the sample film and the other left empty was warmed up to room temperature in a dry N_2 atmosphere to prevent water uptake in the sample.[18] In the meantime, the temperature of the nitrogen-gas filled cryostat was increased to the target annealing temperature (T_{ann} = 319.0, 322.5, or 325.0 K), in order to minimize the time require to stabilize the sample at T_{ann}. After the sample reached room temperature, the IDE cell was quickly mounted in the sample holder and placed into the cryostat. With an average heating rate of 1.2 K/min, the sample temperature approached the target annealing temperature typically in 6–10 min with a temperature overshoot not exceeding 0.2 K. The dielectric measurement was started when the sample temperature was stabilized at the target annealing temperature within a margin better than 0.05 K. Note that each transformation experiment requires a new sample.

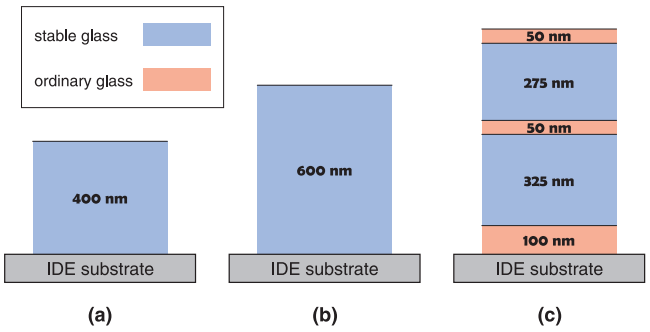

FIG. 1. Schematic representation of the three types of film structures of this study. (a) ultrastable film of 400 nm thickness, (b) ultrastable film of 600 nm thickness, and (c) sequence of conventional and ultrastable glass films totaling 800 nm thickness. The stacked structure of (c) consists of layers of 100, 325, 50, 275, and 50 nm and has a combined thickness of 200 nm (25%) of "conventional" material deposited at $T_{sub} = 0.99\ T_g$ and a total of 600 nm (75%) of ultrastable material deposited at $T_{sub} = 0.85\ T_g$.

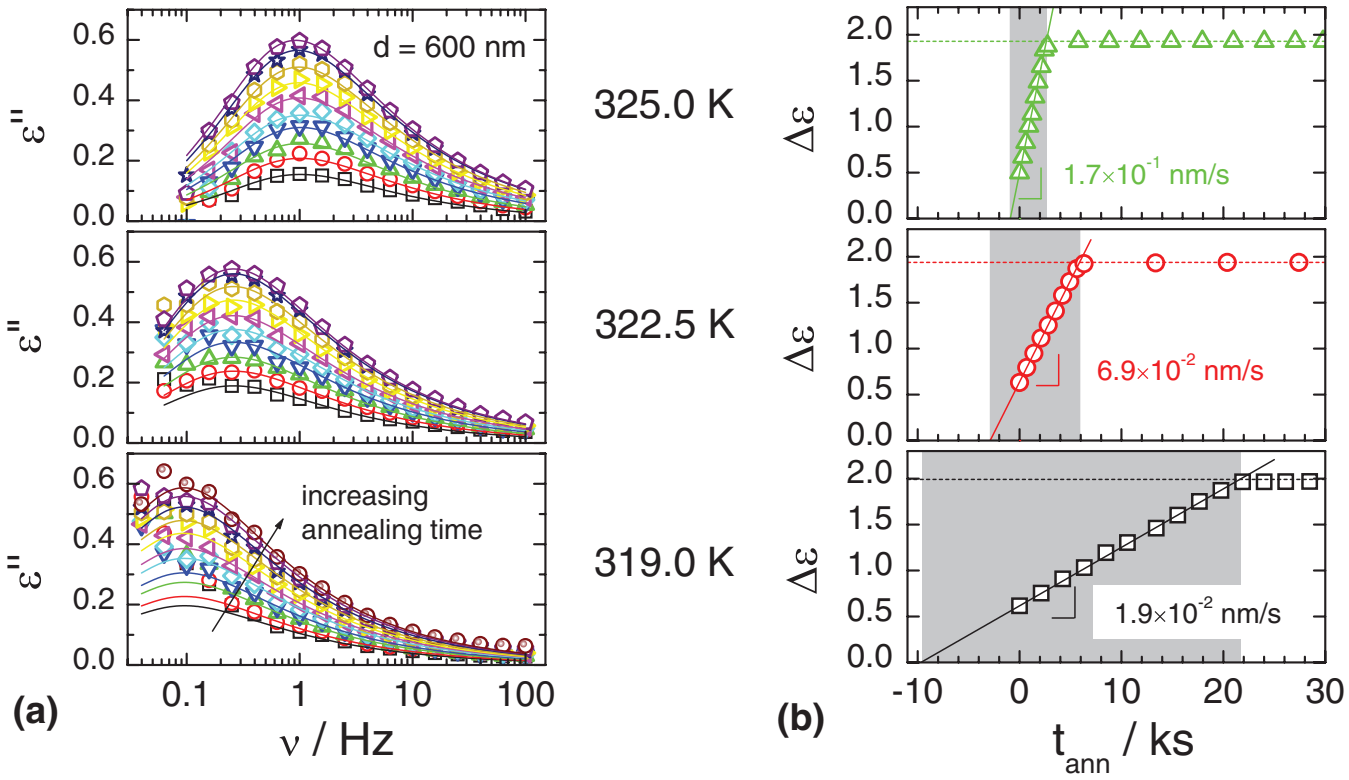

FIG. 2. (a) Dielectric loss spectra of 600 nm ultrastable IMC films at different times when annealed at T_{ann} = 319.0, 322.5, and 325.0 K. Loss amplitudes rise with increasing annealing time. The lines are best HN fits using the same relaxation time (τ_{HN}) and shape parameters (α_{HN},γ_{HN}) that describe the conventional IMC supercooled liquid. (b) The relaxation intensity obtained by HN fitting as a function of time for 600 nm ultrastable IMC films annealed at the same sequence of annealing temperatures. The dashed line shows the value of $\Delta\varepsilon$ for the completely transformed film, the solid lines are linear fits for $\Delta\varepsilon(t_{ann})$ during the transformation, and the area shaded grey indicates the estimated total time scale for the transformation.

The frequency-dependent complex permittivities, $\varepsilon^*(\omega) = \varepsilon'(\omega) - i\varepsilon''(\omega)$, of both IDEs were measured simultaneously using a Solartron 1260 gain-phase analyzer equipped with two Mestec DM-1360 transimpedance amplifiers.[42] For completely transformed IMC films, data were acquired for frequencies in the range from 0.03 Hz to 100 kHz, with the frequencies being logarithmically spaced at a density of 8 per decade. For the measurements monitoring the transformation of the ultrastable IMC films, shorter frequency ranges and a reduced frequency density were employed in order to limit the time required for a frequency scan. The complex permittivity of the IMC film was calculated according to the method described in Ref. 42.

III. RESULTS AND DISCUSSION

The feature responsible for the formation of ultrastable glasses is the high mobility at the glass/vacuum interface during deposition at a temperature somewhat below the conventional T_g; this combination of high mobility and low temperature has not been achieved otherwise.[43,44] Given their exceptional properties, it is not immediately clear whether ultrastable glasses possess the same structure as their conventional liquid or glass counterpart. If the structures differ qualitatively, then the recovery of the equilibrium liquid above T_g could involve a phase transition and the system could display polyamorphism. Ishii *et al.* have reported that such metastable liquid states are responsible for unusual light-scattering properties of *iso*-propylbenzene and ethylbenzene. These optical features were observed immediately following the annealing from the ultrastable glassy state, disappeared after annealing, and remained absent for supercooled liquids formed by cooling the melt.[45,46] Capponi *et al.* reported an analogous feature observed by dielectric spectroscopy.[47] On the other hand, a recent SIMS study[26] suggested that the self-diffusion coefficient D of the liquid transformed from ultrastable IMC glass does not differ from the value of D of the conventional supercooled counterpart. Based on a first order liquid-liquid transition derived from theoretical considerations by Matyushov and Angell,[48] the ultrastable glass to liquid transitions have been viewed as indicators of the existence of thermodynamically different liquid states, at least for fragile systems.[49] In view of the above ambiguity regarding the relevance of different thermodynamic states of the glasses and liquids involved in the studies of ultrastable glasses, a more detailed characterization of the dynamics of samples prepared by the PVD technique is of considerable interest.

A. Transformation of 600 nm ultrastable films at different temperatures

Figure 2(a) shows the dielectric loss spectra of 600 nm vapor-deposited ultrastable IMC films at different times during isothermal annealing at T_{ann} = 319.0, 322.5, and 325.0 K. For all three annealing temperatures, one can see that for the first spectrum recorded the dielectric loss peak is very small

(black squares) and that it gains amplitude in the course of the transformation process, while the spectral position and shape of the loss profile remains annealing invariant. After a certain period of time (see Fig. 2(b)), the dielectric loss spectrum ceases to change regarding its amplitude. At this time, the transformation appears to be completed. Because the determination of $\Delta\varepsilon$ involves the film thickness as a geometrical factor, the relaxation intensities of these films saturate after complete transformation at a common value of $\Delta\varepsilon_{max}$, independent of film thickness. In order to preserve the clarity of the figure, the dielectric loss spectra after the completion of the transformation are not included in Fig. 2(a).

In order to analyze the data of Fig. 2(a) more quantitatively, the dielectric loss curves were subject to fits based upon the empirical Havriliak-Negami (HN) function that is given by[50]

$$\varepsilon^*(\omega) = \varepsilon_\infty + \frac{\Delta\varepsilon}{[1 + (i\omega\tau_{HN})^{\alpha_{HN}}]^{\gamma_{HN}}}, \quad (1)$$

where the shape parameters α_{HN} and γ_{HN} quantify the symmetric and asymmetric broadening, respectively, $\Delta\varepsilon = \varepsilon_s - \varepsilon_\infty$ is the relaxation intensity with ε_s and ε_∞ being the static dielectric constant and dielectric constant in the high-frequency limit, respectively, and τ_{HN} is the characteristic relaxation time which quantifies the structural relaxation time τ_α. A key feature of the fit process is that the parameters τ_{HN}, α_{HN}, and γ_{HN} were kept constant with their values being equivalent to those used for the conventional supercooled state of IMC, i.e., only the relaxation intensity $\Delta\varepsilon$ was used as adjustable parameter. At the temperatures relevant for the present transformation studies, the profile shape is given by $\alpha_{HN} = 0.88$ and $\gamma_{HN} = 0.54$. The resulting fits are included in Fig. 2(a) as solid lines, which provide accurate descriptions of the dielectric loss curves.

As mentioned in the Introduction, the ultrastable IMC film is characterized by a higher density and lower enthalpy. In this ultrastable glassy state, the α-relaxation time is shifted far outside the frequency window of the current dielectric experiment, and no measurable dielectric loss is expected until the onset of the ultrastable glass/liquid transformation. If the temperature could be increased from $T < T_g$ to the annealing temperature $T = T_{ann}$ very rapidly and if the time required to record a spectrum was negligible compared with the transformation time at T_{ann}, then we would expect to observe $\Delta\varepsilon = 0$ for the first spectrum. Accordingly, the observed signals are entirely attributed to the liquid that had been transformed from the ultrastable glass, and the relaxation amplitude of that liquid can be considered an indicator of the volume fraction of material in the liquid state. Since τ_{HN}, α_{HN}, and γ_{HN} are equivalent to those of the conventional supercooled state of IMC formed by cooling the melt, the first measurable component of the liquid transformed from the ultrastable IMC has the same dynamics as that of the conventional supercooled IMC. In other words, the liquid immediately produced by transforming the ultrastable IMC is conventional supercooled IMC, which is consistent with the result of the recent SIMS study.[26]

Figure 2(b) shows the time dependence of the relaxation intensity $\Delta\varepsilon$ of the ultrastable IMC films annealed at T_{ann} = 319.0, 322.5, and 325.0 K. For all three temperatures, one can see that $\Delta\varepsilon$ increases linearly with time and then remains constant. Because $\Delta\varepsilon$ is proportional to the volume of the transformed IMC, the linear dependence of $\Delta\varepsilon$ on time during the transformation process is consistent with the transformation of the ultrastable IMC by a growth front mechanism with a constant propagation velocity. (Because the growth fronts are considered parallel to the electric field line, glass and liquid components act as parallel capacitances and Maxwell Wagner effects remain insignificant.[51–53]) Although small, dielectric loss peaks can already be observed when $t = 0$, which means part of the ultrastable IMC has transformed into liquid when the dielectric measurement is started. This should be due to the finite rate of the temperature ramp, which takes up to 10 min to stabilize the temperature, and/or overnight transportation and storage of the samples. Assuming a loss free ultrastable glassy state, we can assume that the extrapolated "ideal" start point of the transformation should be at the moment when $\Delta\varepsilon = 0$, and that the end point is the moment when $\Delta\varepsilon$ levels off (the crossover point shown in Fig. 2(b)). Accordingly, we extrapolate the linear dependence of $\Delta\varepsilon$ on time to the point when $\Delta\varepsilon = 0$, and the time scale that covers the "ideal" start point through the end point (displayed in Fig. 2(b) as the area shaded grey) is the estimated total transformation time. The transformation times thus obtained are t_{trans} = 31 200 ± 200 s, 8750 ± 50 s, and 3520 ± 30 s for the cases of T_{ann} = 319.0 K, 322.5 K, and 325.0 K, respectively.

By comparing the peak loss frequencies in Fig. 2(a) with the transformation times in Fig. 2(b), one can observe that the temperature dependence $t_{trans}(T)$ parallels that of the dielectric (structural) relaxation time, $\tau_\alpha(T)$, to a good approximation. The actual offset of $t_{trans}(T)$ from $\tau_\alpha(T)$ is depicted in Fig. 3, and amounts to four orders of magnitude, i.e.,

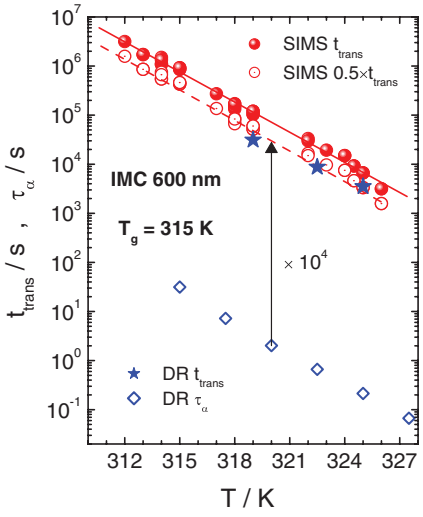

FIG. 3. Stars represent the transformation times, t_{trans}, of the 600 nm ultrastable IMC films as a function of the annealing temperature as derived from the results of Fig. 2(a). Closed and open circles reflect t_{trans} values calculated from the SIMS studies, Ref. 26, with the assumption of one and two growth fronts, respectively. The lines are linear fits to the SIMS results. The structural relaxation times of the conventional liquid from Ref. 42 are shown in terms of dielectric peak relaxation times, τ_α, as diamonds. The arrow indicates that t_{trans} is approximately equal to 10^4 τ_α.

$t_{trans} \approx 10^4\ \tau_\alpha$. In Fig. 3 we also compare the transformation times determined in this work with the result of a recent SIMS study.[26] Although the transformation time of 600 nm ultrastable IMC films has been determined previously by some other methods,[12,13] the only study that used PVD conditions comparable to our present cases is the recent SIMS study.[26] The solid and open circles in Fig. 3 represent the transformation times calculated from the growth front velocity measured in the SIMS experiment, using the assumptions that there are one and two growth fronts, respectively. As can be seen, our result is more consistent with a two growth front pattern, implying that there might be a second growth front at the ultrastable glass/substrate interface for the ultrastable IMC films deposited on the IDE cells.

B. Transformation times for different film configurations

To gain more insight into the transformation process and the propagation speed of the growth front, we also measured the dielectric behavior of 400 nm ultrastable IMC films and 800 nm ultrastable/conventional stacked IMC films during annealing at $T_{ann} = 322.5$ K and 325.0 K. Due to the level of dc-conductivity at lower temperatures for these films, the $T = 319.0$ K case is disregarded in this section. The configuration of the 800 nm ultrastable/conventional mixture IMC film is schematically illustrated in Fig. 1(c), with each ultrastable IMC layer being sandwiched by two conventional IMC glass films. Since the liquid transformed from the ultrastable IMC is actually conventional supercooled IMC liquid, each conventional/ultrastable IMC interface will behave like a growth front during the annealing process, as has been demonstrated in recent experiments.[54] Accordingly, we expected four growth fronts in this configuration, one from each conventional/ultrastable glass interface.

Figure 4(a) shows the dielectric behavior of 400 nm ultrastable IMC, 600 nm ultrastable IMC, and 800 nm stacked IMC films during annealing at 322.5 K. Although these films are different in thickness and/or configuration, one can notice that the dielectric loss peak position is the same for all film configurations (see Fig. 1) at a common temperature of 322.5 K. This is confirmed by the best HN fits shown as lines in Fig. 4(a), which also indicate that the values of the shape parameters α_{HN} and γ_{HN} as well as the time constant τ_{HN} are the same for the three cases and consistent with the conventional liquid counterparts. A similar result was also obtained from the measurements on films with these structures during annealing at 325 K (not shown). As above, the results suggest that the liquid transformed from the ultrastable IMC is conventional SCL, already in the early stages of the transformation process.

The relaxation intensity at different annealing times during the transformation process, $\Delta\varepsilon(t_{ann})$, was obtained from the HN fit parameters, which is plotted against time in Fig. 4(b), analogous to Fig. 2(b). The growth front mechanism suggested for ultrastable glass films of IMC with thick-

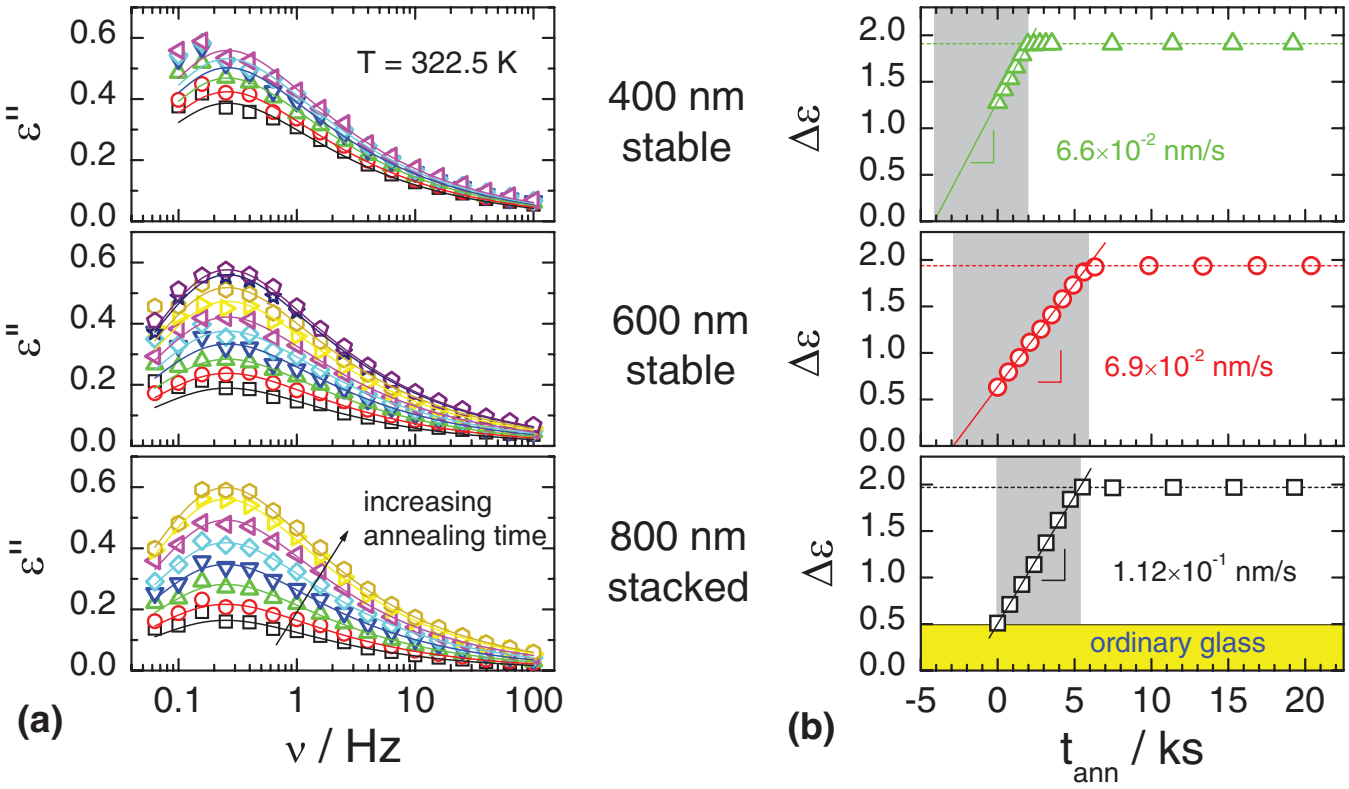

FIG. 4. (a) Dielectric spectra of 400 nm ultrastable IMC, 600 nm ultrastable IMC, and 800 nm stacked IMC films (see Fig. 1) at different times during annealing at 322.5 K. (b) Time dependence of the relaxation intensity, $\Delta\varepsilon(t_{ann})$, for the same three films. The dashed line shows the value of $\Delta\varepsilon$ for the completely transformed film, the solid lines are linear fits for $\Delta\varepsilon(t_{ann})$ during the transformation, and the area shaded grey indicates the estimated total time scale for the transformation. In the lower panel, the yellow area represents the initial relaxation intensity generated from the conventional IMC layers.

ness not exceeding 1 μm implies that the transformation time is proportional to film thickness,[13] because the velocity of the growth front was found to be constant irrespective of the thickness. In the cases of 400 nm and 600 nm ultrastable IMC glass films, the slopes determined by linear fits of $\Delta\varepsilon$ vs time during the transformation process translate into overall conversion rates of 6.6×10^{-2} nm/s and 6.9×10^{-2} nm/s, respectively. Because these two films have the same configuration and thus the same number of growth fronts, the quantitative similarity of these two rates indicates that the velocity of the growth front is independent of film thickness. The transformation time in the 400 nm ultrastable IMC film can be similarly obtained as described above, which is 6040 $\pm$ 50 s, and hence about 2/3 of the transformation time of the 600 nm film.

For the 800 nm conventional/ultrastable glass stacked IMC film, the "ideal" start point of the transformation should be at $\Delta\varepsilon = \Delta\varepsilon_{max}/4$ (200 nm/800 nm) rather than at $\Delta\varepsilon = 0$, because there is a 200 nm conventional IMC liquid layer prior to transformation. The yellow area shown in the lower panel of Fig. 4(b) represents the relaxation intensity generated from that initial conventional supercooled IMC layer, which accounts for 25% of the total film thickness. The transformation time thus spans the time from $\Delta\varepsilon = \Delta\varepsilon_{max}/4$ to $\Delta\varepsilon_{max}$, as indicated by the area shaded grey in the lower panel in Fig. 4(b). The transformation time is determined to be 5360 $\pm$ 50 s, which is about 40% shorter than that of the 600 nm ultrastable IMC film. This means the transformation in the 800 nm mixture IMC film is about 1.65 times faster than in the 600 nm purely ultrastable IMC film, even though both films have the same total thickness of ultrastable IMC material. The slope determined by the linear fit gives a value of 1.1×10^{-1} nm/s for the conversion velocity, also about 1.65 times larger than the 600 nm film without conventional glass layers. When the same IMC films are annealed at 325 K, we found a similar result, with the transformation rate in the 800 nm mixture IMC film being 1.66 times larger than that in the 600 nm ultrastable IMC (not shown). The larger transformation rate in the 800 nm stacked IMC film is readily explained by its larger number of growth fronts. In combination with the previous result that the transformation time of the 600 nm ultrastable IMC case is equivalent to that determined by SIMS measurement when assuming two growth fronts, we now have reason to believe that there are two growth fronts active during the transformation process for the ultrastable IMC films deposited on the IDE cell. Compared with the *in situ* measurements in which the silicon substrate is usually not observed to trigger a growth front,[26] the current finding may be the result of the surface properties of the borosilicate substrate used here or due to temperature fluctuations during sample transport. For the present *ex situ* experiments, we assume that both the free surface and the IDE substrate/ultrastable glass interface can trigger a growth front, implying 2 growth fronts for the cases in Figs. 1(a) and 1(b), and 4 growth fronts for the situation outlined in Fig. 1(c). This would lead to the expectation of a transformation rate that is about a factor of two higher for the 800 nm film compared with the 600 nm case, in reasonable agreement with the factor of 1.65 observed here.

C. Dielectric behavior of completely transformed IMC

Finally, we take a more detailed look at the dielectric behavior of transformed IMC ultrastable glasses. After the annealing measurements discussed above, the IMC film is completely transformed into the supercooled liquid state, with no indication of a residual glassy film above T_g. Analogous to the protocol applied to the conventional IMC film (generated by PVD with a substrate temperature of 0.99 T_g), we cooled the completely transformed IMC film to a temperature slightly below T_g, and then measured the dielectric relaxation behavior while stepwise increasing the temperature. These measurements were carried out after every annealing experiment, and the results are basically the same, irrespective of the annealing history and the configuration of the films.

Figure 5 compares the dielectric permittivity and loss of the completely transformed IMC (lines) with that of the conventional IMC (symbols) in a temperature range from 315 K to 350 K. The same results are obtained for the comparison of all three sample configurations of Fig. 1 with the 600 nm thick conventional IMC case. The dielectric data of the conventional supercooled IMC film are taken from our previous work,[42] which are also measured by the dual-channel impedance measurement setup on differential IDE cells. As can be seen, their dielectric relaxation behavior is practically identical. Relative to the comparison with the data taken during the transformation process, Fig. 5 covers a wider frequency and temperature range.

We also found that the values of the HN parameters obtained by fitting the spectra of the transformed IMC are practically identical to those found for the conventional IMC at all investigated temperatures. Since no systematic difference between transformed IMC and conventional IMC regarding their relaxation characteristics is found, we again conclude

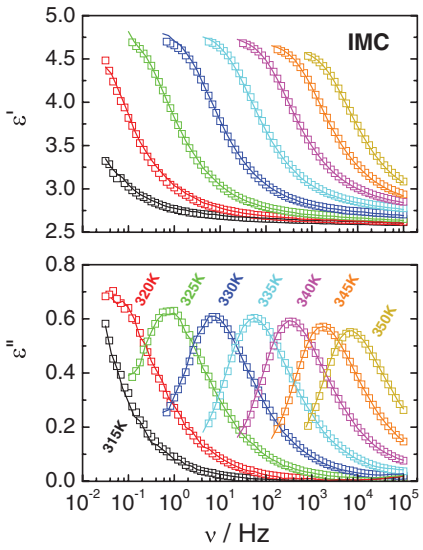

FIG. 5. Comparison of the dielectric permittivity (ε') and loss (ε'') of a 600 nm IMC film prepared in the conventional liquid state (symbols) and a 400 nm ultrastable IMC film after complete transformation to the supercooled liquid (lines). In each panel, separate curves are for different temperatures between 315 K and 350 K as indicated. The same results are obtained for the other sample configurations shown in Figs. 1(b) and 1(c).

that the liquid produced from complete transformation of the ultrastable IMC is in the same liquid state as the supercooled IMC obtained from cooling the melt. Based on the first spectrum recorded during transformation for the 600 nm ultrastable film at $T_{ann} = 325$ K (see Fig. 2), the conventional supercooled liquid behavior is recovered already in the early stages of the transformation process, i.e., when 25% of the material has been transformed, equivalent to a liquid layer of 150 nm total thickness.

IV. SUMMARY AND CONCLUSIONS

Dielectric measurements were carried out to monitor the dynamics of ultrastable glasses of indomethacin during (and after) isothermal annealing for temperatures slightly above the glass transition temperature, $T_g = 315$ K. Films of different thicknesses between 400 and 800 nm have been studied at annealing temperatures ranging from 319 to 325 K. By inserting layers of conventional IMC glass, the effect of the number of growth fronts could also be investigated. The main feature of these experiments is the capability to measure ultrastable glass/liquid conversion rates and to assess the primary relaxation dynamics in terms of complete dielectric loss spectra as layers of IMC liquid are recovered from the ultrastable glassy material.

During annealing, the liquid volume fraction derived from the relaxation amplitude, $\Delta\varepsilon$, increases linearly with time and the total transformation time exceeds the structural relaxation times by a factor of about 10^4, consistent with results from other experimental techniques. An analysis of the loss peaks recorded during this transformation process reveals that the relaxation time τ_α as well as the dispersion shape parameters α_{HN} and γ_{HN} remain constant and equal to their conventional supercooled liquid counterparts. This holds already for the first 150 nm of a liquid layer formed in a 600 nm film, suggesting that the ultrastable IMC glass transforms directly into the well known supercooled liquid state. The linear rise of the relaxation intensity and the observed transformation times are consistent with the constant velocity growth front mechanism observed earlier by SIMS measurements.

Note that a less than ultrastable glass prepared by conventional aging is expected to recover by a gradual softening process, the signature of which is a shift of the primary loss peak from very low frequencies towards the equilibrium value without significant change in amplitude. The present results clearly exclude such a transformation scenario. Future studies might determine whether a glass will choose such a different route to equilibrium if kinetic facilitation originating from interfaces or "defect sites" was completely absent.

Regarding the possible existence of intermediate metastable liquid states that occur during the transformation process, a considerable lifetime of such a state and sufficiently different dynamics relative to the conventional liquid are required for the dielectric experiment to observe such a state. The present experiments would have detected an intermediate state with a mobility three times that of the conventional liquid, a case that had been discussed previously.[24] We also anticipate that if IMC behaved analogous to what has been reported for *iso*-propylbenzene or ethylbenzene,[45,46] our experiments would have provided an indication for a metastable liquid that differs from the conventional supercooled liquid. *In situ* dielectric measurements of *iso*-propylbenzene during its transformation could clarify the potential existence of polyamorphism in that system.

ACKNOWLEDGMENTS

This material is based upon work supported by the National Science Foundation under Grant No. CHE-1012124.

[1] S. F. Swallen, K. L. Kearns, M. K. Mapes, Y. S. Kim, R. J. McMahon, M. D. Ediger, T. Wu, L. Yu, and S. Satija, Science **315**, 353 (2007).
[2] K. L. Kearns, S. F. Swallen, M. D. Ediger, T. Wu, and L. Yu, J. Chem. Phys. **127**, 154702 (2007).
[3] K. L. Kearns, S. F. Swallen, M. D. Ediger, T. Wu, Y. Sun, and L. Yu, J. Phys. Chem. B **112**, 4934 (2008).
[4] L. Zhu and L. Yu, Chem. Phys. Lett. **499**, 62 (2010).
[5] E. Leon-Gutierrez, G. Garcia, M. T. Clavaguera-Mora, and J. Rodriguez-Viejo, Thermochim. Acta **492**, 51 (2009).
[6] M. Ahrenberg, E. Shoifet, K. R. Whitaker, H. Huth, M. D. Ediger, and C. Schick, Rev. Sci. Instrum. **83**, 033902 (2012).
[7] E. Leon-Gutierrez, A. Sepúlveda, G. Garcia, M. T. Clavaguera-Mora, and J. Rodriguez-Viejo, Phys. Chem. Chem. Phys. **12**, 14693 (2010).
[8] K. L. Dawson, L. A. Kopff, L. Zhu, R. J. McMahon, L. Yu, R. Richert, and M. D. Ediger, J. Chem. Phys. **136**, 094505 (2012).
[9] K. L. Dawson, L. Zhu, L. A. Kopff, R. J. McMahon, L. Yu, and M. D. Ediger, J. Phys. Chem. Lett. **2**, 2683 (2011).
[10] K. L. Kearns, K. R. Whitaker, M. D. Ediger, H. Huth, and C. Schick, J. Chem. Phys. **133**, 014702 (2010).
[11] Z. Fakhraai, T. Still, G. Fytas, and M. D. Ediger, J. Phys. Chem. Lett. **2**, 423 (2011).
[12] K. J. Dawson, L. Zhu, L. Yu, and M. D. Ediger, J. Phys. Chem. B **115**, 455 (2011).
[13] K. L. Kearns, M. D. Ediger, H. Huth, and C. Schick, J. Phys. Chem. Lett. **1**, 388 (2010).
[14] S. L. L. M. Ramos, M. Oguni, K. Ishii, and H. Nakayama, J. Phys. Chem. B **115**, 14327 (2011).
[15] S. S. Dalal, A. Sepúlveda, G. K. Pribil, Z. Fakhraai, and M. D. Ediger, J. Chem. Phys. **136**, 204501 (2012).
[16] K. L. Kearns, T. Still, G. Fytas, and M. D. Ediger, Adv. Mater. **22**, 39 (2010).
[17] S. S. Dalal and M. D. Ediger, J. Phys. Chem. Lett. **3**, 1229 (2012).
[18] K. J. Dawson, K. L. Kearns, M. D. Ediger, M. J. Sacchetti, and G. D. Zografi, J. Phys. Chem. B **113**, 2422 (2009).
[19] S. Léonard and P. Harrowell, J. Chem. Phys. **133**, 244502 (2010).
[20] S. Singh and J. J. de Pablo, J. Chem. Phys. **134**, 194903 (2011).
[21] S. F. Swallen, K. Traynor, R. J. McMahon, and M. D. Ediger, Phys. Rev. Lett. **102**, 065503 (2009).
[22] S. F. Swallen, K. L. Kearns, S. Satija, K. Traynor, R. J. McMahon, and M. D. Ediger, J. Chem. Phys. **128**, 214514 (2008).
[23] K. L. Kearns, S. F. Swallen, M. D. Ediger, Y. Sun, and L. Yu, J. Phys. Chem. B **113**, 1579 (2009).
[24] S. F. Swallen, K. Windsor, R. J. McMahon, M. D. Ediger, and T. E. Mates, J. Phys. Chem. B **114**, 2635 (2010).
[25] K. Whitaker, M. Ahrenberg, C. Schick, and M. D. Ediger, J. Chem. Phys. **137**, 154502 (2012).
[26] A. Sepúlveda, S. F. Swallen, L. A. Kopff, R. J. McMahon, and M. D. Ediger, J. Chem. Phys. **137**, 204508 (2012).
[27] S. F. Swallen, K. Traynor, R. J. McMahon, M. D. Ediger, and T. E. Mates, J. Phys. Chem. B **113**, 4600 (2009).
[28] S. F. Swallen and M. D. Ediger, Soft Matter **7**, 10339 (2011).
[29] R. S. Smith, J. Matthiesen, and B. D. Kay, J. Chem. Phys. **132**, 124502 (2010).
[30] A. J. Kovacs, J. Polym. Sci. **30**, 131 (1958).
[31] P. Lunkenheimer, R. Wehn, U. Schneider, and A. Loidl, Phys. Rev. Lett. **95**, 055702 (2005).
[32] X. Shi, A. Mandanici, and G. B. McKenna, J. Chem. Phys. **123**, 174507 (2005).
[33] A. Sepúlveda, E. Leon-Gutierrez, M. Gonzalez-Silveira, M. T. Clavaguera-Mora, and J. Rodriguez-Viejo, J. Phys. Chem. Lett. **3**, 919 (2012).
[34] P. G. Wolynes, Proc. Natl. Acad. Sci. U.S.A. **106**, 1353 (2009).

[35]C. A. Angell, Physica D **107**, 122 (1997).
[36]J. L. Yarger and G. H. Wolf, Science **306**, 820 (2004).
[37]M. Wübbenhorst, S. Capponi, S. Napolitano, S. Rozanski, G. Couderc, N.-R. Behrnd, and J. Hulliger, Eur. Phys. J. Spec. Top. **189**, 181 (2010).
[38]S. Capponi, S. Napolitano, N. R. Behrnd, G. Couderc, J. Hulliger, and M. Wübbenhorst, J. Phys. Chem. C **114**, 16696 (2010).
[39]F. Kremer and A. Schönhals, *Broadband Dielectric Spectroscopy* (Springer, Berlin, 2003).
[40]G. Justin and A. Guiseppi-Elie, Biomacromolecules **10**, 2539 (2009).
[41]L. Yang, A. Guiseppi-Wilson, and A. Guiseppi-Elie, Biomed. Microdevices **13**, 279 (2011).
[42]Z. Chen, A. Sepúlveda, M. D. Ediger, and R. Richert, Eur. Phys. J. B **85**, 268 (2012).
[43]M. Oguni, H. Hikawa, and H. Suga, Thermochim. Acta **158**, 143 (1990).
[44]K. Takeda, M. Oguni, and H. Suga, Thermochim. Acta **158**, 195 (1990).
[45]K. Ishii, H. Nakayama, and R. Moriyama, J. Phys. Chem. B **116**, 935 (2012).
[46]K. Ishii, Y. Yokoyama, R. Moriyama, and H. Nakayama, Chem. Lett. **39**, 958 (2010).
[47]S. Capponi, S. Napolitano, and M. Wübbenhorst, Nat. Commun. **3**, 1233 (2012).
[48]D. V. Matyushov and C. A. Angell, J. Chem. Phys. **126**, 094501 (2007).
[49]C. A. Angell, in *Structural Glasses and Supercooled Liquids: Theory, Experiment, and Applications*, edited by P. Wolynes and V. Lubchenko (Wiley, Hoboken, 2012).
[50]S. Havriliak and S. Negami, Polymer **8**, 161 (1967).
[51]R. W. Sillars, J. Inst. Electr. Eng. **80**, 378 (1937).
[52]R. Pelster, Phys. Rev. B **59**, 9214 (1999).
[53]R. Richert, Eur. Phys. J. Spec. Top. **189**, 37 (2010).
[54]A. Sepúlveda, S. F. Swallen, and M. D. Ediger, J. Chem. Phys. **138**, 12A517 (2013).